Equivalence between short- and long-distance dispersal in individual animal movement

Danish A. Ahmed[1,*], Naveed Ahmed[1], Sergei V. Petrovskii[2], Joseph D. Bailey[3], Michael B. Bonsall[4], and Phillip J. Haubrock[1,5,6]

[1]Center for Applied Mathematics and Bioinformatics, Department of Mathematics and Natural Sciences, Gulf University for Science and Technology, Kuwait

[2]School of Computing and Mathematical Sciences, University of Leicester, UK

[3]Department of Mathematical Sciences, University of Essex, Colchester, UK

[4]Mathematical Ecology Research Group, Department of Biology, University of Oxford, UK

[5]University of South Bohemia in České Budějovice, Faculty of Fisheries and Protection of Waters, South Bohemian Research Centre of Aquaculture and Biodiversity of Hydrocenoses, Zátiší 728/II, 389 25 Vodňany, Czech Republic

[6]Senckenberg Research Institute and Natural History Museum Frankfurt, Department of River Ecology and Conservation, Gelnhausen, Germany

[*]Corresponding author: Ahmed.D@gust.edu.kw

Keywords: Animal movement, Random walks, Brownian motion, Lévy walks, Dispersal kernels

Abstract

Random walks (RW) provide a useful modelling framework for the movement of animals at an individual level. If the RW is uncorrelated and unbiased such that the direction of movement is completely random, the dispersal is characterised by the statistical properties of the probability distribution of step lengths, or the dispersal kernel. Whether an individual exhibits short- or long-distance dispersal can be distinguished by the rate of asymptotic decay in the end-tail of the distribution of step-lengths. If the decay is exponential or faster, referred to as a thin-tail, then the step length variance is finite – as occurs in Brownian motion. On the other hand, inverse power-law step length distributions have a heavy end-tail with slower decay, resulting in an infinite step length variance, which is the hallmark of a Lévy walk. Although different approaches to relate these different dispersal mechanisms have been used, they are ad hoc and sub-optimal. We provide a more robust method by ensuring that the survival probability, that is the probability of occurrence of steps longer than a fixed characteristic step length is the same for both distributions. Moreover, we derive an optimal value for the survival probability by minimising the $\mathbb{L}^2$-distance between the dispersal kernels. By computing the optimal probability for movement paths with commonly used thin- and heavy-tailed step length distributions, we form equivalence between short- and long-distance dispersal of animals in different spatial dimensions. We also demonstrate how our findings can be applied to ecological scenarios, to more accurately relate dispersal mechanisms within a modelling framework for spatio-temporal population dynamics.

1 Introduction

Understanding the dispersal mechanisms that drive animal movement over multi-spatial scales from local scale foraging and home range exploration to large scale migration, has been a key research focus for ecologists (Bullock et al., 2002; Clobert et al., 2001; Nathan et al., 2008). The virtual ecologist approach where simulations can be used to mimic the movement of real species provides a framework to study fundamental aspects of animal behaviour and movement in a controlled setting (Zurell et al., 2010). By simulating random walks (RW) researchers can gain insights into foraging strategies, searching patterns, and movement decisions (Bartumeus et al., 2005; Bartumeus and Catalan, 2009; James et al., 2011; Viswanathan et al., 2011), how animals

respond to specific cues or stimuli (Reynolds, 2010), and navigate and explore in their environment (Codling and Bode, 2016; Bailey et al., 2018). Moreover, by incorporating RW models into larger ecological frameworks, in combination with other approaches, such as GPS tracking (Cagnacci et al., 2010; Williams et al., 2020) and individual-based modelling (Grimm and Railsback, 2005), researchers can analyse the causes and consequences of movement dispersal on spatial dynamics (Bowler and Benton, 2005; Hooten et al., 2017).

While several mathematical models have been developed to describe the movement dispersal of animals, on an individual level much of the commonly used methodology is derived from discrete-time random walks (Berg, 1983; Turchin, 1998; Codling et al., 2008). For this, an animal's continuous movement path is mapped as a time-series of distinct locations (Turchin, 1998; Grimm and Railsback, 2005), and the discretised movement path is characterised by the probability distributions of step lengths $\lambda(l)$ and turning angles. If the RW is uncorrelated and unbiased which corresponds to Brownian motion, an individual is equally likely to move in each possible direction with no long-term preferred movement direction, and thus movement dispersal solely relies on the statistical properties of $\lambda(l)$ (Lin and Segel, 1974; Okubo, 1980). If the step-length distribution is thin-tailed, that is, the end-tail decays sufficiently fast at long step lengths, then the step length variance exists and is finite, and the RW is classed as scale-specific. A direct consequence is that the mean-squared displacement (MSD) is defined (i.e., the expected value of the squared beeline distance between an individuals' initial and final positions), which is a key metric to analyse movement paths and can be expressed as an exact formula in terms of the number of steps in the walk and the mean-squared step length (Kareiva and Shigesada, 1983). Therefore, any two scale-specific RWs that are parametrised differently can be related by assuming equal MSD (Ahmed et al., 2021b). A specific example of a movement process that has a thin-tailed dispersal kernel is Brownian motion. Ecologists have routinely applied Brownian motion and diffusive dispersal as a null model for animal movement (Skellam, 1973; Kareiva and Shigesada, 1983), with empirical support found in particular for animals moving in resource-rich environments (Bartumeus et al., 2003; De Knegt et al., 2007; Humphries et al., 2010, 2012; Nolet and Mooij, 2002). Also, a more mechanistic approach to the application of Brownian motion in ecological studies has been emphasised, specifically when resources are abundant with Brownian motion being shown to arise from ecological interactions rather than being a default or primary

movement pattern (De Jager et al., 2014).

Another conceptual tool used to model animal movement paths is the Lévy walk (LW) (Viswanathan et al., 2000; Benhamou, 2007; James et al., 2011; Reynolds, 2018). In this case, the end-tail of the step-length distribution decays asymptotically according to an inverse power law, $\lambda(l) \sim l^{-\mu}$, $1 < \mu \leq 3$ with slower decay for smaller μ, which is referred to as a heavy or fat-tail (Petrovskii and Morozov, 2009). The corresponding walk has an infinite step length variance and, being scale-free, is self-similar at various spatial scales (Viswanathan et al., 2000; Reynolds, 2018). In comparison to movement described by thin-tailed distributions, this movement type constitutes long-distance dispersal due to the occurrence of longer steps being more probable as the tails do not decay as quickly. Because of the infinite step length variance, the expected MSD does not exist, and therefore it is less clear how equivalence can be formed between a LW and a scale-specific RW, although a characteristic length scale can always be defined either through the median step length, using geometric-averages, or through dimensional analysis (Kawai and Petrovskii, 2012).

Whether an animal's movement trajectory can be well described by a LW based on observed movement data, can only be accurately detected if the survival distribution of step lengths obeys an inverse power law (Benhamou, 2007). This has been a common approach in several animal movement studies that seek to relate a LW to a scale-specific RW. For instance, in a study on the boundary counts of *Tenebrio molitor* beetles resulting from Brownian or Lévy-type movement, the dispersal kernels were related with $p = 0.1$ (Bearup et al., 2016). Elsewhere, on identifying which movement pattern arising from RWs is faster or more efficient, several probabilities were considered with values $p = 0.1, 0.5$ and 0.9 (Choules and Petrovskii, 2017). Also, in a study on the effect of density-dependent individual movement on spatial pattern formation, $p = 0.9$ was used (Ellis et al., 2018). It is evident that p is arbitrarily chosen, possibly for convenience, however, a unique optimal value can be determined by introducing an additional constraint, that is by minimising the $\mathbb{L}^2$-distance which is the sum of the squares of the differences between the dispersal kernels. In this work, we present the methodology and compute optimal survival probabilities p for individuals exhibiting different modes of dispersal and moving randomly in space. Here we link the concept of a scale-free RW to the existence of the step length variance, forming an equivalence between the LW and scale-specific RW by ensuring that the survival probability p of occurrence of steps, l, longer than some characteristic step length L is the same for both walks, that

is $\mathbb{P}(l > L) = p$.

Studying animal dispersion has been a central focus in movement ecology (Nathan et al., 2008; Hawkes, 2009), and gaining a deeper understanding of how the underlying dispersal mechanisms can be connected contributes to addressing challenges in spatial ecology. This understanding finds application in various ecological contexts, including biodiversity (Jeltsch et al., 2013), nature management and conservation (Allen and Singh, 2016; Fraser et al., 2018), biological invasions (Shigesada and Kawasaki, 1997), ecological monitoring (Petrovskii et al., 2014; Miller et al., 2015) and disease spread (Fofana and Hurford, 2017; Chu et al., 2021).

2 Equivalence between short- and long-distance dispersal in different spatial dimensions

2.1 Movement in 1D space

We begin by considering an individual performing a RW in an isotropic environment in one-dimensional (1D) space. Such a modelling framework provides a conceptual basis and thus useful for developing more realistic ecological models that depict movement phenomena in higher dimensions (Viswanathan et al., 2011; Ellis et al., 2018). If the individual is located at x_{i-1}, then the location x_i at the next step is determined by

$$x_i = x_{i-1} + \Delta x_i, \quad i = 1, 2, 3, ... \tag{2.1}$$

where Δx_i is a random variable for the i^{th} step along the walk with centrally symmetric probability distribution $\phi(\Delta x)$ with zero mean $\mathbb{E}[\Delta x] = 0$. In this case, moving either to the left or right is equiprobable with value $1/2$. The probability of executing a step that exceeds a finite distance L from the individuals current location x_i is given by

$$\mathbb{P}\left(|\Delta x| > L\right) = p, \tag{2.2}$$

where p is the survival probability that lies between 0 and 1. Here, we consider two distinct movement types that characterise short- and long-distance dispersal. First, a thin-tailed step distribution with scale parameter σ and finite variance $\phi_A(\Delta x|\sigma)$, and second, a heavy-tailed distribution with scale parameter γ with infinite variance $\phi_B(\Delta x|\gamma)$. The subscripts A and B are

included to distinguish between these probability distributions.

For the purposes of equivalence, we fix the survival probability p to be the same for both distributions

$$\int_{|\Delta x|>L} \phi_A(\Delta x|\sigma) d\Delta x = \int_{|\Delta x|>L} \phi_B(\Delta x|\gamma) d\Delta x = p, \tag{2.3}$$

and due to symmetry, this can be written as

$$\int_{L}^{\infty} \phi_A(\Delta x|\sigma) d\Delta x = \int_{L}^{\infty} \phi_B(\Delta x|\gamma) d\Delta x = \frac{p}{2}. \tag{2.4}$$

For commonly used step distributions in simulating animal movements in 1D these integrals can be evaluated analytically, and in some cases, by eliminating L it is possible to express the ratio of distribution parameters as a function of p, so that

$$\frac{\gamma}{\sigma} = s(p). \tag{2.5}$$

We compute the sum of the squares of the differences between the probability distributions across their domain, equivalent to finding the $\mathbb{L}^2$-distance. Hence we consider the distance metric $\mathfrak{D}(\phi_B, \phi_A)$ given as

$$\mathfrak{D}(\phi_B, \phi_A) = \int_{-\infty}^{\infty} \left[\phi_B(\Delta x|\gamma) - \phi_A(\Delta x|\sigma)\right]^2 d\Delta x, \tag{2.6}$$

and since these step distributions are centrally symmetric, this can be written as

$$\mathfrak{D}(\phi_B, \phi_A) = 2\int_{0}^{\infty} \left[\phi_B(\Delta x|\sigma s(p)) - \phi_A(\Delta x|\sigma)\right]^2 d\Delta x, \tag{2.7}$$

which is expressed solely in terms of σ and p. To determine the optimal probability p^* we minimise the $\mathbb{L}^2$-distance between these probability distributions, by solving

$$\frac{d\mathfrak{D}}{dp} = 0 \tag{2.8}$$

evaluated at $p = p^*$. Thus distribution parameters can be related from equation (2.5) as $\gamma = s(p^*)\sigma$ with corresponding optimal characteristic scale length L^* from equation (2.4).

2.2 Movement in 2D space

For the more realistic case of individual movement in two-dimensional (2D) space, e.g., terrestrial animals (Bartumeus et al., 2005; Gurarie and Ovaskainen, 2013; Ahmed et al., 2023), the movement path can be considered as a continuous curvilinear trajectory $\mathbf{x}(t) = (x(t), y(t))$ over time t. This movement path can be discretised over time as a series of steps linking an animal's location $\mathbf{x}_{i-1} = (x_{i-1}, y_{i-1})$ at time t_{i-1} to the next location $\mathbf{x}_i = (x_i, y_i)$ at time t_i as

$$\mathbf{x}_i = \mathbf{x}_{i-1} + (\Delta\mathbf{x})_i, \quad i = 1, 2, 3, \ldots \tag{2.9}$$

where $(\Delta\mathbf{x})_i = (\Delta x_i, \Delta y_i)$ is a step vector whose components are random variables, for the i^{th} step along the walk, the distances between any two locations are step lengths $l_i = |\mathbf{x}_i - \mathbf{x}_{i-1}|$, and $t_i = i\Delta t$ where Δt is a constant time increment.

In 2D it is more convenient to describe the RW in polar co-ordinates by expressing the step vector in terms of step lengths l and step orientations θ (or headings), using the transformation

$$\Delta x = l\cos\theta, \quad \Delta y = l\sin\theta, \quad l \geq 0, \quad -\pi < \theta \leq \pi \tag{2.10}$$

with inverse transformation

$$l^2 = (\Delta x)^2 + (\Delta y)^2, \quad \theta = \text{atan}_2\left(\Delta y, \Delta x\right), \tag{2.11}$$

where $\text{atan}_2\left(\Delta y, \Delta x\right) = \arctan\left(\frac{\Delta y}{\Delta x}\right)$ for $\Delta x > 0$ and $\arctan\left(\frac{\Delta y}{\Delta x}\right) \pm \pi$ for $\Delta x < 0$. Here, $\mathbb{E}[l]$ is the mean step length and $\mathbb{E}[v] = \mathbb{E}[l]/\Delta t$ is the mean speed. The turning angle α_i can then be measured as the difference between the orientations of two successive steps

$$\alpha_i = \theta_i - \theta_{i-1}. \tag{2.12}$$

On assuming that step lengths l_i and step orientations θ_i are neither autocorrelated nor cross-correlated (Benhamou, 2006), the individual movement can be simulated once the distributions of step lengths $\lambda(l)$ and turning angles $\omega(\alpha)$ are prescribed. Since our focus is on movement dispersal arising from the properties of $\lambda(l)$, we assume there is no preferred local

or global movement direction, resulting in completely random movement and thus α is uniformly distributed from $-\pi$ to π, as has been observed in various species (Kareiva, 1983; Hapca et al., 2009; De Jager et al., 2012).

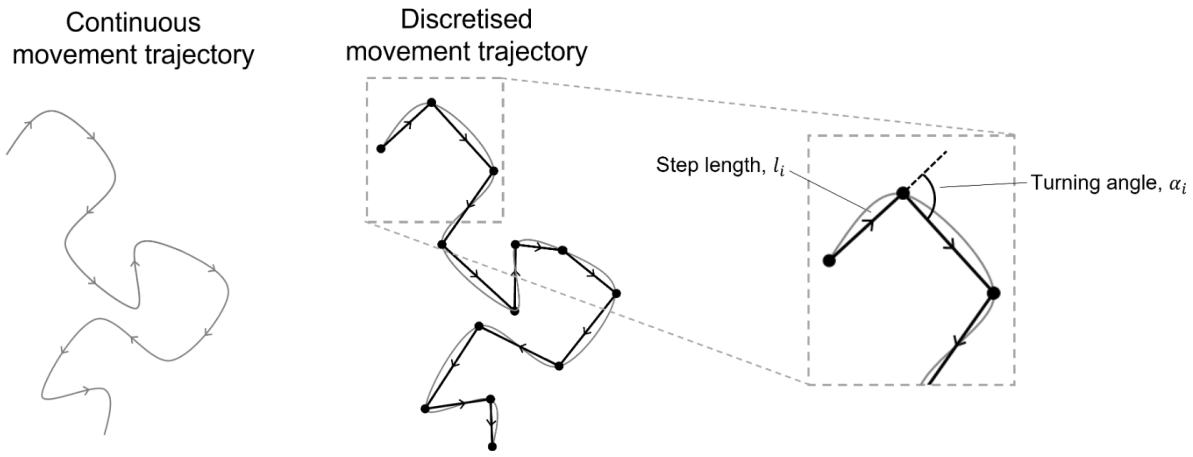

Figure 1: Mapping the continuous movement trajectory of an animal as a series of discrete steps with step lengths l_i and turning angles α_i resulting in the random walk, reproduced from Ahmed et al. (2023).

Now consider two random walkers, the first characterised by a thin-tailed step length distribution $\lambda_A(l|\sigma)$ with scale parameter σ and finite variance, and second, with a heavy-tailed step length distribution $\lambda_B(l|\gamma)$ with scale parameter γ and infinite variance. Since step lengths are non-negatively defined, the survival probability is defined as

$$\mathbb{P}(l > L) = p, \tag{2.13}$$

and on fixing p to be the same for both distributions, one gets

$$\int_L^\infty \lambda_A(l|\sigma)dl = \int_L^\infty \lambda_B(l|\gamma)dl = p. \tag{2.14}$$

The rest of the methodological details are the same as in the 1D case in §2.1, where the optimal survival probability p^* is sought, by minimizing the following $\mathbb{L}^2$-distance between the step length probability distributions

$$\mathfrak{D}(\lambda_B, \lambda_A) = \int_0^\infty [\lambda_B(l|\sigma s(p)) - \lambda_A(l|\sigma)]^2 dl \tag{2.15}$$

with relation between distribution parameters $\gamma = s(p^*)\sigma$ and corresponding optimal characteristic scale length L^* from equation (2.14).

2.3 Movement in 3D space

Many animals make use of space in three-dimensions (3D), such as flying and aquatic animals (Cooper et al., 2014; Cleasby et al., 2015; Aspillaga et al., 2019), as well as some ground-dwelling animals that can move through different altitudes on steep terrains (Tracey et al., 2014). In this case, the discrete-time RW model described by equation (2.9) applies but extended to 3D by including a vertical direction z_i, where an animal executes a step by moving from its current location $\mathbf{x}_{i-1} = (x_{i-1}, y_{i-1}, z_{i-1})$ to the next $\mathbf{x}_i = (x_i, y_i, z_i)$, with step lengths between two successive locations $l_i = |\mathbf{x}_i - \mathbf{x}_{i-1}|$ and random step vector $(\Delta\mathbf{x})_i = (\Delta x_i, \Delta y_i, \Delta z_i)$. Using spherical co-ordinates, the step vector can be expressed in terms of step lengths l, azimuthal angle θ which is equivalent to longitude and the polar angle ξ which is equivalent to co-latitude, using the transformation

$$\Delta x = l\cos(\theta)\sin(\xi),\ \Delta y = l\sin(\theta)\sin(\xi),\ \Delta z = l\cos(\xi), \quad l \geq 0, \quad -\pi < \theta \leq \pi, \quad 0 \leq \xi \leq \pi \tag{2.16}$$

with inverse transformation

$$l = \sqrt{(\Delta x)^2 + (\Delta y)^2 + (\Delta z)^2}, \quad \theta = \operatorname{atan}_2(\Delta y, \Delta x), \quad \xi = \arccos\left(\frac{\Delta z}{l}\right). \tag{2.17}$$

In an isotropic environment, θ is uniformly distributed from $-\pi$ to π, and ξ is half-sine distributed $\frac{1}{2}\sin(\xi)$ with values drawn between 0 and π (e.g., see Ahmed et al. (2020)). Thus in this case, the movement pattern is characterised by the distribution of step lengths $\lambda(l)$. Equivalence between short- or long-distance dispersal in 3D can be obtained using the methodology described in 2D, see §2.2, with the survival probability given by equation (2.13), which is optimised by minimising the $\mathbb{L}^2$-distance in equation (2.15).

3 Equivalence between short- and long-distance dispersal for $\mu = 2$

3.1 1D case with normal and Cauchy step distributions

To demonstrate equivalence between two distinct RWs in 1D, we consider steps to be independently Gaussian (normally) distributed ϕ_{G} which is given as

$$\phi_G(\Delta x|\sigma) = \frac{1}{\sigma\sqrt{2\pi}} \exp\left(-\frac{(\Delta x)^2}{2\sigma^2}\right), \tag{3.1}$$

with zero mean $\mathbb{E}[\Delta x] = 0$ and finite variance σ^2. This distribution is thin-tailed due to the faster than exponential decay in the end tails. Alongside this, consider the Cauchy step distribution ϕ_{C}, which reads

$$\phi_C(\Delta x|\gamma) = \frac{\gamma}{\pi(\gamma^2 + (\Delta x)^2)}, \tag{3.2}$$

which is heavy-tailed due to the slower decay in the end tails according to $\phi_C \sim \frac{1}{(\Delta x)^2}$ as $|\Delta x| \to \infty$, with infinite variance. For these distributions, we can express the characteristic scale length L in terms of the survival probability p by applying equation (2.13), which gives

$$L = \sigma\sqrt{2}\mathrm{erfc}^{-1}(p) = \gamma \tan\left[\frac{\pi(1-p)}{2}\right] \tag{3.3}$$

where $\mathrm{erfc}^{-1}(\tau)$ is the inverse of the complimentary error function defined by $\mathrm{erfc}(\tau) = \frac{2}{\sqrt{\pi}}\int_\tau^\infty \exp(-\tau'^2)d\tau'$. On rearranging the above equation, we can express the ratio of distribution parameters as a function of p only:

$$s(p) = \frac{\gamma}{\sigma} = \sqrt{2}\mathrm{erfc}^{-1}(p)\cot\left[\frac{\pi(1-p)}{2}\right]. \tag{3.4}$$

The $\mathbb{L}^2$-distance is given as

$$\mathfrak{D}(\phi_C, \phi_G) = \frac{1}{\sigma\sqrt{\pi}} \cdot \left[\frac{1}{s\sqrt{\pi}} - 2\sqrt{2}\exp\left(\frac{s^2}{2}\right)\mathrm{erfc}\left(\frac{s}{\sqrt{2}}\right) + 1\right]. \tag{3.5}$$

The optimal survival probability p^* which minimizes this occurs when

$$\frac{d\mathfrak{D}}{dp} = -\frac{s'}{2\pi\sigma\mathfrak{D}}\left[\frac{1-4s^2}{s^2} + 2\sqrt{2\pi}s\exp\left(\frac{s^2}{2}\right)\operatorname{erfc}\left(\frac{s}{\sqrt{2}}\right)\right] = 0, \tag{3.6}$$

which gives $p^* = 0.721$, and is invariant with respect to σ. The distribution parameter ratio is $s^* = 0.762$ and $L^* = 0.357\sigma$ from equation (3.3).

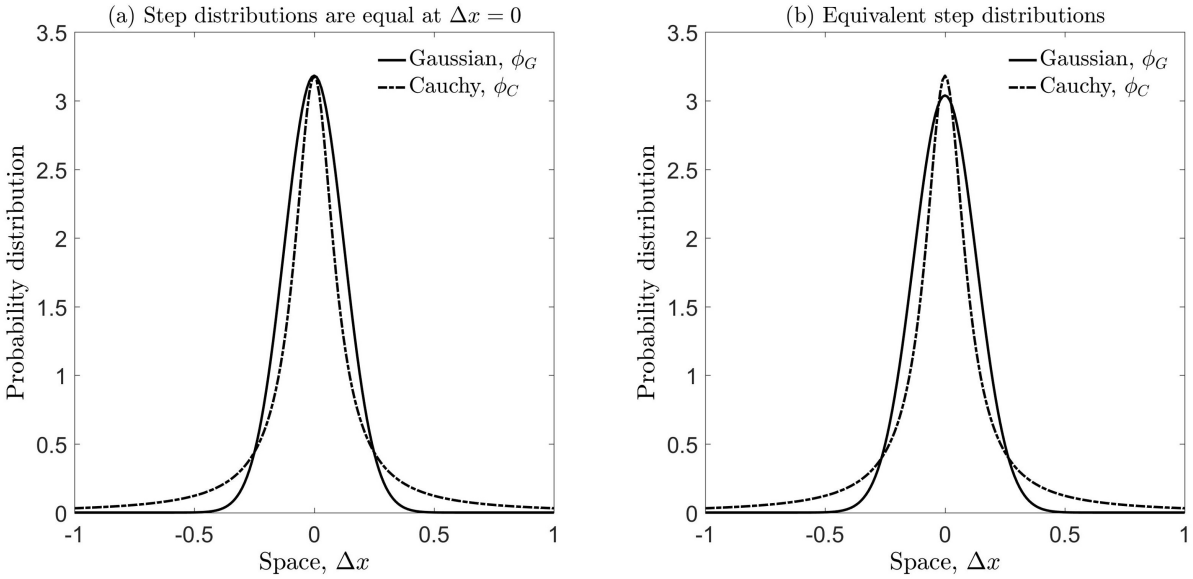

Figure 2: (a) The Gaussian (solid) and the Cauchy (dashed) step distributions. We set $\gamma = 0.1$ and set $\sigma^2 = \frac{\pi\gamma^2}{2}$ to ensure agreement between the two probability distributions at $x = 0$. (b) Equivalent step distributions with optimal survival probability $p^* = 0.721$. Illustration in (a) adapted from Figure 5.2 in Lutscher (2019), but used therein in the context of dispersal kernels.

For movement in 1D space, when examining the Gaussian step distribution depicted in Figure 2 (a) and (b), an initial observation suggests a subtle distinction. Yet, this seemingly minor difference can result in a considerable effect on the ensuing movement process. In scenario (b), characterised by an optimal relationship between the step distributions, the Gaussian distribution exhibits a higher frequency of longer steps, rendering it more akin to the Cauchy distribution. This is counterbalanced by a reduced peak. Therefore, a more precise comparison can be made among animals that may disperse following Brownian motion or engage in long-distance dispersal.

3.2 2D case with Rayleigh and folded-Cauchy step length distributions

Consider a 2D RW with random step vector $(\Delta\mathbf{x}) = (\Delta x, \Delta y)$ whose components are independently distributed according to a zero-centered normal distribution $\phi_G(\Delta x)$ and $\phi_G(\Delta y)$ with the same finite variance σ^2, see equation (3.1). It can be derived that the corresponding step length distribution is the Rayleigh distribution λ_R, which reads

$$\lambda_R(l) = \frac{l}{\sigma^2}\exp\left(-\frac{l^2}{2\sigma^2}\right), \tag{3.7}$$

with mean step length $\mathbb{E}(l) = \frac{\sigma\sqrt{2\pi}}{2}$ and finite variance $2\sigma^2\left(1-\frac{\pi}{4}\right)$, see Petrovskii et al. (2014). The resulting movement type is a discrete-time model of Brownian motion (Turchin, 1998; Petrovskii et al., 2012). Alternatively, consider a folded-Cauchy step-length distribution λ_{fC}, which reads

$$\lambda_{fC}(l|\gamma) = \frac{2\gamma}{\pi(\gamma^2 + l^2)}, \tag{3.8}$$

with quadratic decay in the end tail according to $\lambda_{fC} \sim \frac{1}{l^2}$ as $l \to \infty$, with infinite variance. The characteristic scale length L can be expressed in terms of the survival probability p to get

$$L = \sigma\sqrt{-2\ln p} = \gamma\tan\left[\frac{\pi}{2}(1-p)\right], \tag{3.9}$$

and on rearranging this, the ratio of distribution parameters is

$$s(p) = \frac{\gamma}{\sigma} = \sqrt{-2\ln p}\cot\left[\frac{\pi}{2}(1-p)\right]. \tag{3.10}$$

The $\mathbb{L}^2$-distance between these step length distributions is

$$\mathfrak{D}(\lambda_{fC}, \lambda_R) = \frac{1}{\pi\sigma}\cdot\left(\frac{1}{s} - 2s\exp\left(\frac{s^2}{2}\right)\mathrm{E}_1\left(\frac{s^2}{2}\right) + \frac{\pi\sqrt{\pi}}{4}\right), \tag{3.11}$$

where $\mathrm{E}_1(\tau) = \int_\tau^\infty \frac{1}{\tau'}\exp(\tau')d\tau'$ is a form of the exponential integral. The optimal survival probability is a solution of

$$\frac{d\mathfrak{D}}{dp} = -\frac{s'}{2\pi\sigma\mathfrak{D}}\left[\frac{1-4s^2}{s^2} + 2\left(1+s^2\right)\exp\left(\frac{s^2}{2}\right)\mathrm{E}_1\left(\frac{s^2}{2}\right)\right] = 0, \tag{3.12}$$

which gives $p^* = 0.658$, with distribution parameter ratio $s^* = 1.536$ and $L^* = 0.915\sigma$ from equation (3.9).

3.3 Equivalent boundary counts in 2D space

Figure 3 illustrates two equivalent RWs based on the formulation in §3.2, (a) for short-distance dispersal with Rayleigh step length distribution and $\sigma = 0.5$, and (b) for long-distance dispersal with folded-Cauchy step length distribution $\mu = 2$ and $\gamma = s^*\sigma = 0.768$. For this choice of σ, the probability $p^* = 0.658$ of executing a step of length greater than $L^* = 0.458$ is the same for both walks.

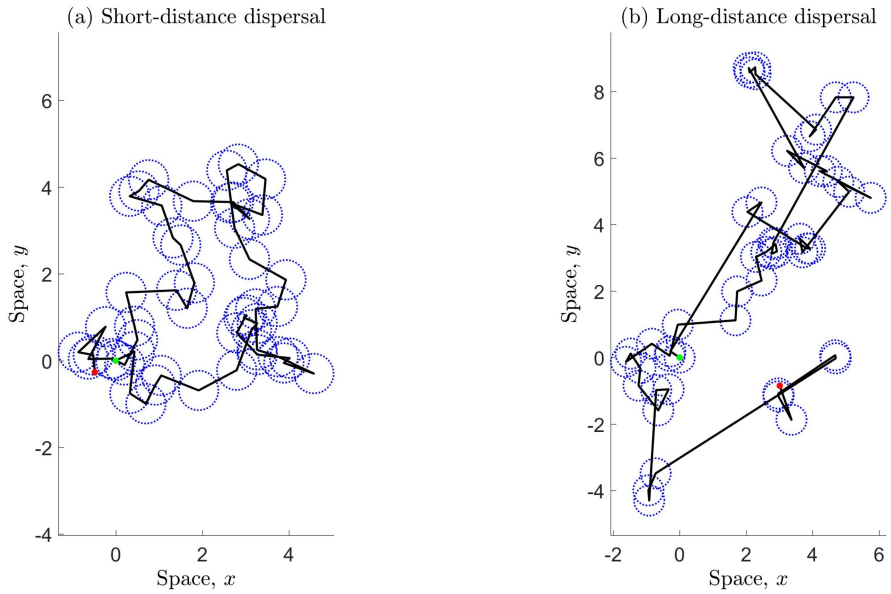

Figure 3: Equivalence between short- and long-distance dispersal in 2D space. (a) RW with Rayleigh distributed step lengths with $\sigma = 0.5$, and (b) RW with folded-Cauchy distributed step lengths with $\gamma = 0.768$. The ratio of distribution parameters is $s^* = 1.536$ with optimal survival probability $p^* = 0.658$. Both RWs satisfy the condition $\mathbb{P}(l > L^*) = p^*$, with the characteristic scale length $L^* = 0.458$ (radius of dashed circles at each location). Each individual starts at the origin (green marker) and the walk terminates after executing 50 steps (red marker).

Consider a population of N individuals with initial location uniformly distributed over a small circular vicinity of radius L^*. The movement of each individual in the population is modelled by a RW, with either a thin-tailed distribution of step lengths representing short-distance dispersal (black dots), and in another scenario with heavy-tailed for long-distance dispersal (red dots), Fig. 4a-c. The proportion of individuals which exit the region are recorded after each step in the walk.

This proportion is the same irrespective of the distribution of step lengths, as both movement types are deemed equivalent, Fig. 4d.

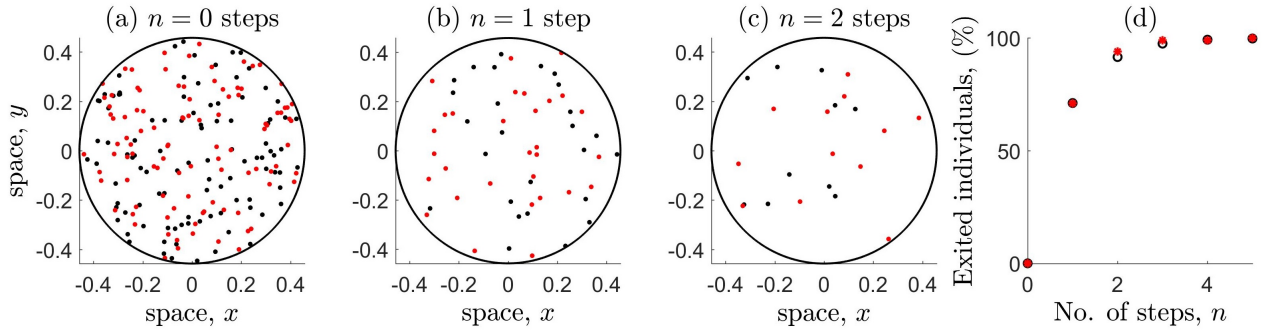

Figure 4: Equivalent exit counts. (a)-(c) Spatial distribution of a population of $N = 100$ individuals performing a RW with Rayleigh step length distribution (thin-tail) with scale parameter $\sigma = 0.5$ (black dots), and on the same circular region of radius $L^* = 0.458$, a population of $N = 100$ individuals performing a RW with folded-Cauchy step length distribution (heavy end-tail) with scale parameter $\gamma = 0.768$ (red dots). These RWs are equivalent in the sense that $\mathbb{P}(l > L^*) = p^*$ is the same for both walks with optimal survival probability $p^* = 0.658$ computed by minimising the the $\mathbb{L}^2$-distance between these step-length distributions. (d) Proportion (%) of individuals that exit the domain for each type of walk, with short-distance dispersal (thin end-tail, black circles), and long-distance dispersal (heavy end-tail, red markers).

3.4 3D case with chi and folded-Cauchy step length distributions

For Brownian motion in 3D space the step increments $(\Delta\mathbf{x}) = (\Delta x, \Delta y, \Delta z)$ are independently distributed according to a zero-centered normal distribution with the same finite variance, see equation (3.1). In this case the variable l/σ follows a chi distribution with three degrees of freedom, corresponding to step length distribution λ_χ, given as

$$\lambda_\chi(l|\sigma) = \frac{2l^2}{\sigma^3\sqrt{2\pi}} \exp\left(-\frac{l^2}{2\sigma^2}\right), \tag{3.13}$$

with mean step length $\mathbb{E}(l) = 4\sigma/\sqrt{2\pi}$ and finite variance $3\sigma^2\left(1 - \frac{8}{3\pi}\right)$, see Ahmed et al. (2020).

If we also consider the folded-Cauchy step length distribution λ_{fC} in equation (3.8), the characteristic scale length L can be related to the survival probability p as

$$L = \sigma\sqrt{2I^{-1}\left(p, \frac{3}{2}\right)} = \gamma\tan\left[\frac{\pi}{2}(1-p)\right] \tag{3.14}$$

where $I^{-1}(\tau, a)$ is the inverse of the upper incomplete gamma function, defined as $I(\tau, a) =$

$\frac{1}{\Gamma(a)}\int_\tau^\infty (\tau')^{a-1}e^{-\tau'}d\tau'$. On re-arranging equation (3.14) we have

$$s(p) = \frac{\gamma}{\sigma} = \sqrt{2I^{-1}\left(p, \frac{3}{2}\right)}\cot\left[\frac{\pi}{2}(1-p)\right]. \tag{3.15}$$

We can compute an analytic expression for the $\mathbb{L}^2$-distance as

$$\mathfrak{D}(\lambda_{fC}, \lambda_\chi) = \frac{1}{\sigma\sqrt{\pi}} \cdot \left[\frac{1-4s^2}{s\sqrt{\pi}} + 2\sqrt{2}s^2 \exp\left(\frac{s^2}{2}\right)\operatorname{erfc}\left(\frac{s}{\sqrt{2}}\right) + \frac{3}{4}\right], \tag{3.16}$$

with optimal survival probability p^* as a solution of

$$\frac{d\mathfrak{D}}{dp} = -\frac{s'}{2\pi\sigma\mathfrak{D}}\left[\left(\frac{1}{s}+2s\right)^2 - 2\sqrt{2\pi}s(2+s^2)\exp\left(\frac{s^2}{2}\right)\operatorname{erfc}\left(\frac{s}{\sqrt{2}}\right)\right] = 0, \tag{3.17}$$

which gives $p^* = 0.650$, with distribution parameter ratio $s^* = 2.089$, with $L^* = 1.282\sigma$ from equation (3.14).

4 Equivalence between short- and long-distance dispersal for general exponent μ

4.1 1D case with normal and power law step distributions

We consider two distinct RWs in 1D space where the probability distributions of the step increments are normally distributed $\phi_G(\Delta x)$, and alternatively distributed according to a power law

$$\phi_P(\Delta x|\gamma,\mu) = \frac{A}{(\gamma+|\Delta x|)^\mu}, \quad A = \frac{1}{2}(\mu-1)\gamma^{\mu-1}, \quad 1 < \mu \leq 3, \tag{4.1}$$

where γ is the distribution scale parameter and A is a normalisation constant. This is a is heavy-tailed distribution with infinite variance, and the rate of decay in the end tails is $\phi_P \sim \frac{1}{|\Delta x|^\mu}$ as $|\Delta x| \to \infty$, with faster decay for larger exponent μ. Applying the condition $\mathbb{P}(l > L) = p$ for both of these distributions, the characteristic scale length L can be expressed in terms of the survival probability p as

$$L = \sigma\sqrt{2}\operatorname{erfc}^{-1}(p) = \gamma\left(p^{\frac{1}{1-\mu}} - 1\right) \tag{4.2}$$

and on eliminating L the ratio of distribution parameters is

$$s(p|\mu) = \frac{\gamma}{\sigma} = \frac{\sqrt{2}\text{erfc}^{-1}(p)}{p^{\frac{1}{1-\mu}} - 1}. \tag{4.3}$$

The $\mathbb{L}^2$-distance between these probability distributions ϕ_P and ϕ_G is

$$\mathfrak{D}(\phi_P, \phi_G) = \frac{2}{\sigma^2}\int_0^\infty \left[\frac{\mu - 1}{2s\left(1 + \frac{\Delta x}{\sigma s}\right)^\mu} - \frac{1}{\sqrt{2\pi}}\exp\left(-\frac{(\Delta x)^2}{2\sigma^2}\right)\right]^2 d\Delta x. \tag{4.4}$$

Let $\zeta = \frac{\Delta x}{\sigma}$, the integral becomes

$$\mathfrak{D}(\phi_P, \phi_G) = \frac{2}{\sigma}\int_0^\infty \left[\frac{\mu - 1}{2s\left(1 + \frac{\zeta}{s}\right)^\mu} - \frac{1}{\sqrt{2\pi}}\exp\left(-\frac{\zeta^2}{2}\right)\right]^2 d\zeta. \tag{4.5}$$

The $\mathbb{L}^2$-distance is scaled by a factor of $1/\sigma$, and therefore decreases with larger σ, but is minimised at some optimal probability p^* which is independent of σ. This integral is not analytically tractable, but can be evaluated using numerical integration techniques such as the trapezoidal rule.

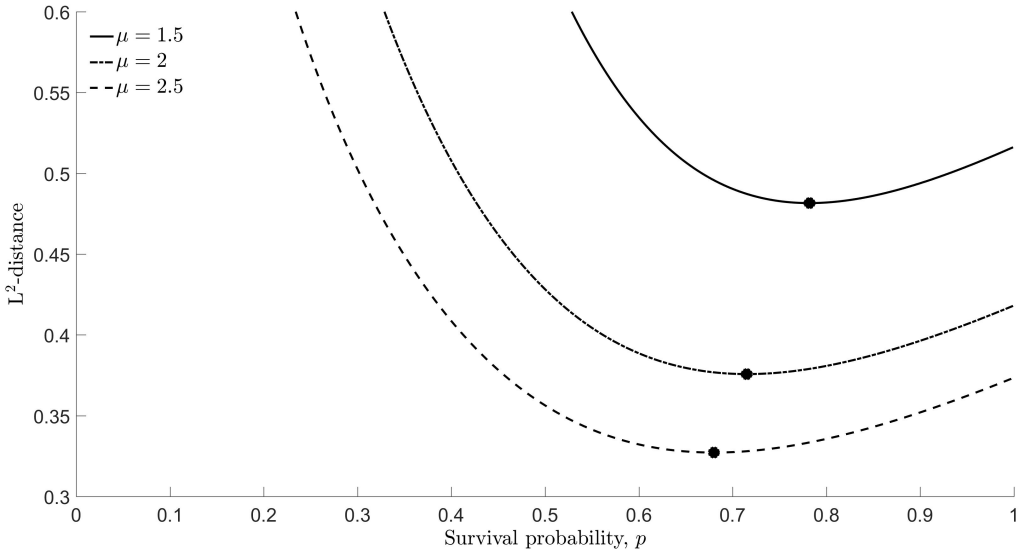

Figure 5: Plot of the $\mathbb{L}^2$-distance between the step distributions ϕ_P and ϕ_G with $\sigma = 0.5$ as a function of the survival probability p, for different heavy-tail exponents $\mu = 1.5, 2, 2.5$. The markers depict the minimum point in each case, that is the optimal probability p^* at which the $\mathbb{L}^2$-distance is minimised $\mathfrak{D}^*$. For $\mu = 1.5$, $\mathfrak{D}^* = 0.482$ at $p^* = 0.782$, for $\mu = 2$, $\mathfrak{D}^* = 0.376$ at $p^* = 0.715$ and for $\mu = 2.5$, $\mathfrak{D}^* = 0.327$ at $p^* = 0.680$.

Fig. 5 illustrates that the $\mathbb{L}^2$-distance is minimised with optimal probability $p^* = 0.782$ for $\mu = 1.5$, $p^* = 0.715$ for $\mu = 2$, and $p^* = 0.680$ for $\mu = 2.5$. Therefore p^* decreases with faster decay in the end tails. Equivalence can be sought between two 1D RWs with normal and power law step distributions by relating distribution parameters through the ratios $s^* = \gamma/\sigma = 0.435, 0.916, 1.407$, respectively, with corresponding length scales $L^* = 0.277\sigma, 0.365\sigma, 0.412\sigma$ determined by equation (4.2). In the case of (b), we obtain the same value of p^* on relating the normal and Cauchy ($\mu = 2$) step distributions in §3.1, which implies that in this case, the shape of the distribution is not important.

4.2 2D case with Rayleigh and Pareto step length distributions

Consider the movement of two individuals performing a RW in 2D space, with step length distributions given by the Rayleigh distribution $\lambda_R(l)$ in equation (3.7) and a Pareto distribution with general exponent μ given by

$$\lambda_P(l|\gamma,\mu) = \frac{A}{(\gamma+l)^\mu}, \quad A = (\mu-1)\gamma^{\mu-1}, \quad 1 < \mu \leq 3, \tag{4.6}$$

where γ is the distribution parameter and A is a normalizing constant. The distribution is heavy-tailed with rate of decay $\lambda_P \sim \frac{1}{l^\mu}$ as $l \to \infty$, and has an infinite variance. Using the definition of the survival probability $\mathbb{P}(l > L) = p$ for both distributions, we obtain

$$L = \sigma\sqrt{-2\ln p} = \gamma\left(p^{\frac{1}{1-\mu}} - 1\right) \tag{4.7}$$

with ratio of distribution parameters

$$s(p|\mu) = \frac{\gamma}{\sigma} = \frac{\sqrt{-2\ln p}}{p^{\frac{1}{1-\mu}} - 1}. \tag{4.8}$$

The $\mathbb{L}^2$-distance between these probability distributions λ_P and λ_R is

$$\mathfrak{D}(\lambda_P, \lambda_R) = \int_0^\infty \left[\frac{\mu - 1}{\sigma s\left(1 + \frac{l}{\sigma s}\right)^\mu} - \frac{l}{\sigma^2}\exp\left(-\frac{l^2}{2\sigma^2}\right)\right]^2 dl, \tag{4.9}$$

and by introducing a change of variables by re-scaling step lengths $\zeta = \frac{l}{\sigma}$, this can be written as

$$\mathfrak{D}(\lambda_P, \lambda_R) = \frac{1}{\sigma}\int_0^\infty \left[\frac{\mu - 1}{s\left(1 + \frac{\zeta}{s}\right)^\mu} - \zeta\exp\left(-\frac{\zeta^2}{2}\right)\right]^2 d\zeta, \tag{4.10}$$

which decreases with an increase in σ. The optimal probability p^* which minimises the $\mathbb{L}^2$-distance can be computed numerically, see later Table 1.

4.3 3D case with chi and Pareto step length distributions

For movement in 3D space, consider the following step length distributions, chi λ_χ in equation (3.13) and Pareto λ_P in equation (4.6). In this case the characteristic scale length is

$$L = \sigma\sqrt{2I^{-1}\left(p, \frac{3}{2}\right)} = \gamma\left(p^{\frac{1}{1-\mu}} - 1\right) \tag{4.11}$$

with ratio of distribution parameters

$$s(p|\mu) = \frac{\gamma}{\sigma} = \frac{\sqrt{2I^{-1}\left(p, \frac{3}{2}\right)}}{p^{\frac{1}{1-\mu}} - 1}. \tag{4.12}$$

The $\mathbb{L}^2$-distance between λ_χ and λ_P is

$$\mathfrak{D}(\lambda_\chi, \lambda_P) = \int_0^\infty \left[\frac{\mu - 1}{\sigma s \left(1 + \frac{l}{\sigma s}\right)^\mu} - \frac{2l^2}{\sigma^3\sqrt{2\pi}} \exp\left(-\frac{l^2}{2\sigma^2}\right) \right]^2 dl, \tag{4.13}$$

and with re-scaled step lengths $\zeta = \frac{l}{\sigma}$, this reads

$$\mathfrak{D}(\lambda_\chi, \lambda_P) = \frac{1}{\sigma} \int_0^\infty \left[\frac{\mu - 1}{s\left(1 + \frac{\zeta}{s}\right)^\mu} - \frac{2\zeta^2}{\sqrt{2\pi}} \exp\left(-\frac{\zeta^2}{2}\right) \right]^2 d\zeta, \tag{4.14}$$

with optimal probability p^* that minimises this $\mathbb{L}^2$-distance computed numerically, see Table 1.

4.4 Ansatz function for the optimal survival probability

We compute the optimal probabilities p^* whilst considering varying heavy-tail exponents μ, for movement in 1D, 2D and 3D space for step length distributions considered in §4.1 normal and power law, §4.2 Rayleigh and Pareto, and §4.3 chi and Pareto, Table 1.

μ	1D	2D	3D	μ	1D	2D	3D
1.1	0.919	0.908	0.902	2.1	0.707	0.709	0.705
1.2	0.867	0.858	0.852	2.2	0.699	0.702	0.698
1.3	0.831	0.824	0.817	2.3	0.692	0.696	0.692
1.4	0.804	0.798	0.792	2.4	0.686	0.690	0.687
1.5	0.782	0.777	0.772	2.5	0.680	0.686	0.682
1.6	0.764	0.761	0.755	2.6	0.675	0.681	0.677
1.7	0.749	0.747	0.742	2.7	0.670	0.677	0.673
1.8	0.736	0.735	0.730	2.8	0.666	0.673	0.670
1.9	0.725	0.725	0.721	2.9	0.662	0.670	0.666
2.0	0.715	0.717	0.712	3.0	0.658	0.666	0.663

Table 1: Optimal survival probabilities p^* for varying exponents μ, for movement in different spatial dimensions.

The values of p^* are approximately the same irrespective of the spatial dimension, because in

either case, the LW movement type is compared to Brownian motion i.e., Gaussian increments are considered in each dimension. We propose the following Ansatz function

$$p^*(\mu) = \frac{c_0(\mu-1)+1}{c_1(\mu-1)+1}, \quad c_1 = \frac{2c_0+1}{p^*(3)} - \frac{1}{2}, \quad 1 < \mu \leq 3 \tag{4.15}$$

to express p^* as a function of μ, which depends on a single parameter c_0, and c_1 is expressed in terms of c_0 and $p^*(3)$, which is the optimal probability for $\mu = 3$, see Table 1. We find that there is a non-linear relationship, where p^* decreases with an increase in μ, i.e., for heavy-tailed distributions with end tail(s) that decays at a much faster rate.

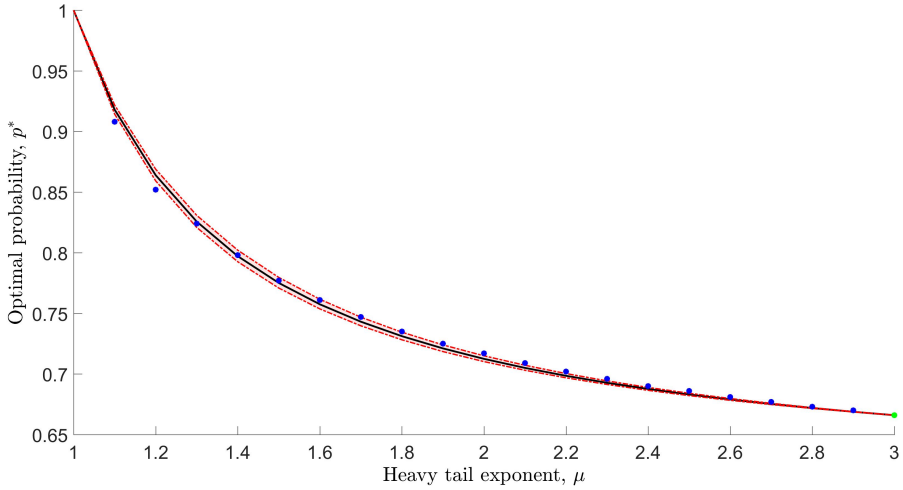

Figure 6: The ansatz function given by equation (4.15) (solid curve) is fitted for optimal probabilities p^* as a function of the exponent μ, computed for movement in 2D space with Power law and Rayleigh step length distributions (circle markers). The non-linear regression curve fitting tool 'lsqcurvefit' from Matlab was used to estimate the best fit parameter $c_0 = 1.561$, with $p^*(3) = 0.666$ from Table 1 and $c_1 = 2.594$ computed from (4.15). The shaded area enveloped by the dashed curves is a 99% confidence region for the range of c_0, which lies between 1.438 and 1.684. The goodness of fit is quantified by the coefficient of determination $R^2 = 0.995$ and the root mean square error $RMSE = 0.004$.

5 Equivalence between dispersal kernels

Integro-difference equations (IDEs) provide a useful modelling framework to describe the spatio-temporal dynamics of a population (Kot and Schaffer, 1986; Andersen, 1991; Neubert et al., 1995), and has advantages over other approaches (e.g., diffusion-reaction models, Holmes et al. (1994); Okubo and Levin (2001)) due to the ability to capture more complex spatial dynamics,

non-local interactions, and various dispersal processes.

The governing equation reads

$$N_{t+1}(\mathbf{r}) = \int_{\Omega} \lambda(\mathbf{r},\mathbf{r}')F(N_t(\mathbf{r}'))d\mathbf{r}' \tag{5.1}$$

where N_t is the population density in year t, $F(.)$ is a growth function that describes the ecological mechanisms and processes that underlie the growth dynamics (Sandefur, 2018), and $\lambda(\mathbf{r},\mathbf{r}')$ is the dispersal kernel which gives the probability distribution of the event that an individual located before dispersal at position $\mathbf{r}' = (x',y')$ moves after dispersal to the position $\mathbf{r} = (x,y)$ over a dispersal domain Ω (Lewis et al., 2006; Lutscher, 2019). Here, our focus is on the rate of spread in the population which depends on the properties of the dispersal kernel. Assuming that dispersal is homogeneous and isotropic so that the probability of moving from $\mathbf{r}$ to $\mathbf{r}'$ depends only on the distance r between the two positions, it follows that $\lambda(\mathbf{r},\mathbf{r}') = \lambda(|\mathbf{r}-\mathbf{r}'|)$, where $r = |\mathbf{r}-\mathbf{r}'| = \sqrt{(x-x')^2+(y-y')^2}$.

Here we consider several dispersal kernels with different properties, and aim to form equivalence between the thin-tailed 2D Gaussian kernel described by

$$\lambda_G(r,\theta) = \frac{1}{2\pi\sigma^2}\exp\left(-\frac{r^2}{2\sigma^2}\right) \tag{5.2}$$

and heavy-tailed kernels, when the probability distribution of moving over distance r has a power law tail, that is $r\lambda(r,\theta) \sim r^{-\mu}$ for large r, with exponent $\mu = 2$. Specifically, consider the 2D Cauchy type I kernel, given by

$$\lambda_{C_1}(r,\theta) = \frac{\gamma_1}{\pi(\gamma_1+r)^3} \tag{5.3}$$

and the 2D Cauchy type II kernel

$$\lambda_{C_2}(r,\theta) = \frac{\gamma_2}{2\pi(\gamma_2^2+r^2)^{\frac{3}{2}}}. \tag{5.4}$$

To form a condition of equivalence between the thin- and different heavy-tailed dispersal kernels, consider the probability p of finding an individual after the dispersal exceeding a distance of radius a.

For the Gaussian kernel, we have that

$$P(r > a) = \int_0^{2\pi} \int_a^{\infty} \lambda_G(r,\theta) r dr d\theta = p, \tag{5.5}$$

and on computing this, we obtain the radius a as a function of p,

$$a = \sigma\sqrt{-2\ln p} \tag{5.6}$$

as previously seen in equation (3.9) for the Rayleigh probability distribution.

Similarly, for the Cauchy type dispersal kernels, we have that

$$P(r > a_i) = \int_0^{2\pi} \int_{a_i}^{\infty} \lambda_{C_i}(r,\theta) r dr d\theta = p, \quad i = 1,2, \tag{5.7}$$

On evaluating this, we obtain for the Cauchy type I kernel

$$a_1 = \gamma_1 \cdot \left(\frac{\sqrt{1-p}}{1-\sqrt{1-p}} \right) \tag{5.8}$$

and for the Cauchy type II kernel

$$a_2 = \gamma_2 \cdot \frac{\sqrt{1-p^2}}{p}. \tag{5.9}$$

Given the same fixed radius in either case $a_1 = a$ and $a_2 = a$, on equating (5.6) with (5.8) and (5.9) separately, we obtain a relationship between the dispersal kernel parameters as a function of p, given as

$$s_1(p) = \frac{\gamma_1}{\sigma} = \sqrt{-2\ln p}\left(\frac{1}{\sqrt{1-p}} - 1 \right), \quad s_2(p) = \frac{\gamma_2}{\sigma} = p\sqrt{\frac{-2\ln p}{1-p^2}}. \tag{5.10}$$

It is precisely the $\mathbb{L}^2$-distance between the dispersal kernels

$$\mathfrak{D}(\lambda_{C_i}, \lambda_G) = 4\pi^2 \int_0^{\infty} \left[r\lambda_{C_i}(r,\theta) - r\lambda_G(r,\theta) \right]^2 dr, \quad i = 1,2. \tag{5.11}$$

that is

$$\mathfrak{D}(\lambda_{C_1}, \lambda_G) = \frac{1}{\sigma} \int_0^{\infty} \left[\frac{2s_1(p)r}{(s_1(p)+r)^3} - r\exp\left(-\frac{r^2}{2} \right) \right]^2 dr, \tag{5.12}$$

and

$$\mathfrak{D}(\lambda_{C_2}, \lambda_G) = \frac{1}{\sigma}\int_0^\infty \left[\frac{s_2(p)r}{(s_2^2(p)+r^2)^{\frac{3}{2}}} - r\exp\left(-\frac{r^2}{2}\right)\right]^2 dr, \tag{5.13}$$

with $\gamma_i = \sigma s_i(p)$, that we seek to minimise to obtain an optimal probability p^*. The radius at where this occurs can be determined from equation (5.8) for a fixed value of σ. Although the $\mathbb{L}^2$-distance can be written in exact form by evaluating the integrals in equations (5.12)-(5.13), the expression is quite bulky and complicated (i.e., involves the Meijer G-function) and thus we resort to numerical integration. We find that the dispersal kernels are equivalent for the Gaussian vs. Cauchy type I case with optimal probability $p^* = 0.718$ with $s_1 = 0.719$, $a_1 = 0.814\sigma$, and for the Gaussian vs. Cauchy type II case with $p^* = 0.727$ with $s_2 = 0.845$, $a_2 = 0.799\sigma$.

6 Discussion

Much has been discussed in the literature regarding the existence of power laws in the step lengths of animal movements as well as the statistical approaches used to identify such distributions (Edwards et al., 2007; Plank and Codling, 2009; Auger-Méthé et al., 2011; Breed et al., 2015). Whilst debate for the reality of power law behaviour continues, it is clear that observed data has been shown to demonstrate traits of such heavy-tailed distributions (Reynolds, 2014). Our work here demonstrates that a property of these heavy-tailed distributions, namely their potential for long-distance dispersal, can be replicated by a simple adjustment to the parameter of the thin-tailed exponential distribution. This is of significance in various movement ecological settings, as the diffusion capability of individual movement has been identified as being an important and appropriate measure in determining dispersal capability (Bearup et al., 2016), with applications in population dispersal (Gurarie et al., 2009; Hapca et al., 2009), individual interactions and contact rates (Bailey, 2023), the spread of diseases (Fofana and Hurford, 2017; Ahmed et al., 2021a), pest monitoring (Petrovskii et al., 2014; Banks et al., 2020), and foraging behaviour (Humphries et al., 2010; James et al., 2011). Below we detail two ecological settings in which the work presented here has an immediate application.

6.1 Boundary counts

Building on the work of Bearup et al. (2016), who demonstrated that in terms of boundary counts of a population of individuals, the heavy-tailed power law distribution is expected to become clearly indistinguishable from Brownian motion with thin-tailed step length distribution, for values of the exponent μ in the power law being less than 2.5. Here, it has been shown that these two methods can become almost indistinguishable for higher values of μ over small arenas, demonstrated by considering the case of $\mu = 2$ with optimal survival probability $p^* = 0.658$ in Figure 4, when the precise step-length distribution of the Brownian motion is altered. Thus, despite variations in decay rates at the tail of the step-length distribution, various movement patterns are essentially similar, if our focus is on the probability of departing from an arena or habitat of a specific size. The close relationship between these distinct movement modes, highlights that accurately inferring between the thin- and heavy-tailed distributions requires careful and considered approaches, which may also be dependent upon the experimental setting.

In other ecological scenarios, distinguishing between step length distributions with different tails is seldom achievable for two primary reasons: (1) the data is typically characterised by high levels of noise (Breed et al., 2015), and (2) long-distance relocations are inherently rare, making it challenging to reveal the tail. Furthermore, the question arises as to whether animals really adhere to any of these refined distributions such as exponential or power law (Benhamou, 2007). In this context, the concept of establishing equivalence between different step length distributions offers a solution. Essentially, if our interest lies solely in the probability of leaving or staying in a domain of a certain size, there is no imperative need to make such distinctions. The conditions for equivalence operate optimally, in fact precisely, within specific spatial scales and for certain survival probabilities. This insight could lay the groundwork for a more effective design, such as in the case of nature protection areas. Additionally, it hints at a potential evolutionary strategy, suggesting the existence of mechanisms that have led to these characteristic spatial scales and survival probabilities.

6.2 Biological invasions

The introduction of non-native species is recognised as a significant threat to global ecosystems. They detrimentally impact economies (Diagne et al., 2021), the environment, and native species thereby deteriorating ecosystem functioning, which often leads to substantial biodiversity loss and human well-being (Courchamp et al., 2017). Biological invasions are the directed, human-mediated transportations and subsequent releases of species (either intentionally or unintentionally) beyond their native biogeographical boundaries from which they can potentially spread (Simberloff, 2013; Pyek et al., 2020). This process can be conceptualised in four phases: (1) a species is intentionally or unintentionally transported to a new area through human activities, or naturally dispersing after a barrier is removed or made permeable through human action. (2) In the new region, it escapes or is willingly introduced into (evolutionary) novel locations (3) where it establishes a viable (i.e., self-sustaining) population and (4) spreads (Shigesada and Kawasaki, 1997; Blackburn et al., 2011). While the latter two stages occur with or without direct human assistance, the quality, quantity, and frequency of introductions (i.e., generally termed 'propagule pressure') are relevant at all stages (e.g., Lockwood et al. (2013); Briski et al. (2014)). The concept of 'spread' in invasion ecology is therefore important because it describes to the movement and dispersal of a non-native species beyond its original point of introduction (Hui and Richardson, 2017; Wilson et al., 2008), forming the basis for the classifications of non-native populations as 'invasive' (Soto et al., 2023). Also, a better understanding of invasive spread is crucial to validating and improving theoretical models that predict spatial patterns resulting from biological invasions (Hastings, 1996; Lewis et al., 2016).

A mathematical description of the invasion process is traditionally with the application of reaction-diffusion equations (Bouin et al., 2012, 2018; Morris et al., 2019; Keenan and Cornell, 2021). Nevertheless, some have adopted an alternative framework, namely integro-difference equation (IDE) formulations, because they explicitly account for the species distinct dispersal and growth phases, and accommodate for various movement behaviours, including those exhibiting non-Gaussian characteristics (e.g., see Lutscher (2019)). In practical terms, the dispersal kernel can be determined directly through field observations, including mark-recapture, trap count, or movement data, or it can be formulated based on the fundamental physical or behavioural processes

that govern movement (Skarpaas and Shea, 2007; Butikofer et al., 2018). Typical choices of the dispersal kernel that are frequently used in calculations are thin-tailed distributions such as the Gaussian or Laplace kernels (e.g., insect dispersal, Neubert et al. (1995)), or where dispersal distances follow a power law decay such as the Cauchy kernel (Shaw, 1995).

Moreover, several authors have applied these IDE models to problems in invasion biology and related the dispersal kernels. For example, on investigating the patchy invasion spread of non-native species by short- and long-distance dispersal, Rodrigues et al. (2015) formulated an IDE model based on the movement of two interacting predator-prey species in 2D space. They formed a condition of equivalence between the thin- and heavy-tailed dispersal kernels by setting a radius a within which the probability of finding an individual after the dispersal is set at an arbitrary value of $p = 0.5$ (which is the same as the probability of exceeding this distance). However, our approach improves upon this, by providing methods to compute an optimal probability p^* as demonstrated in §5. We found that for the dispersal kernels considered in Rodrigues et al. (2015), in the (a) Gaussian vs. Cauchy type I case, $p^* = 0.718$, with ratio of dispersal kernel parameters $s_1 = \gamma_1/\sigma = 0.719$ and characteristic radial length $a_1 = 0.814\sigma$, and in the (b) Gaussian vs. Cauchy type II case, $p^* = 0.727$, $s_2 = \gamma_2/\sigma = 0.845$, $a_2 = 0.799\sigma$. Contrast this to the sub-optimal condition of equivalence formed in Rodrigues et al. (2015) with $p = 0.5$, $s_1 = (2-\sqrt{2})\sqrt{\ln 2} \approx 0.488$, and $s_2 = \sqrt{(2\ln 2)/3} \approx 0.680$, with same radius $a_1 = a_2 = \sigma\sqrt{2\ln 2} \approx 1.177\sigma$. How the pattern of invasive species spread depicted by the prey spatial distributions in Rodrigues et al. (2015) may change with these different parameter values, and what are the implications on the results requires further analysis.

6.3 Implications of diffusive and super-diffusive animal movement is context dependent

Animal movement in general and animal dispersal in particular are fundamental phenomena that have significant effect on many aspects of population dynamics and ecosystem functioning (Turchin, 1998; Bullock et al., 2002). Peculiarities of animal movement – in particular, whether they can be regarded as diffusive or super-diffusive – has been a focus of intense debate for almost three decades (Viswanathan et al., 2011). In spite of many questions remaining, there is sufficient evidence that at least some of the individuals of some species can, under certain conditions, perform the movement that is better classified as super-diffusive, e.g., Lévy flights or Lévy walks,

rather than diffusive, usually referred to as Brownian motion (Sims et al., 2019).

What is often forgotten in that debate is the ecological context: whatever is the movement type, what are the implications for the corresponding ecosystem and/or how does it affect the function that the given species has inside the ecological community? Super-diffusively moving animals would normally have a fat-tailed dispersal kernel (Kot et al., 1996), which apparently means a higher proportion of long-distance dispersers. In turn, larger dispersal distances may have a significant effect on the properties of both the given species and the ecosystem as a whole, e.g. enhancing spread of infectious diseases (Mundt et al., 2009), facilitating synchronisation between population fluctuations in different habitats (Blomfield et al., 2023), etc. There can, however, be other contexts or implications where not the forerunners but the main bulk of the population is more important. One example is given by invertebrate animals trapping for monitoring purposes, with the goal to estimate the corresponding population density (Petrovskii et al., 2012, 2014). In this case, the effect of forerunners is limited to the special case of monitoring at the edge of the advancing invasion front, i.e., where the population density is very low; however, fast dispersers hardly have any significant effect on trap counts after the population settles down.

As another important example, there is growing evidence that animals, especially large animals, act as a vector transporting (with dung and bodies) nutrients across space, in particular phosphorus that is a limiting factor in many ecosystems (Doughty et al., 2013, 2016). Arguably, in such a case it is not the number and speed of the forerunners that matters but the typical distance that describes the movement of the bulk of the population. In turn, shifting the focus away from the forerunners has immediate implications for the choice of modelling framework. For instance, instead of more complicated modelling approaches based on integral-difference or integral-differential equations that can be sensitive to details of the dispersal kernel (which is usually difficult to restore from the data with sufficient accuracy, cf. De Jager et al. (2012); Jansen et al. (2012), a simpler and more robust approach based on the diffusion equation can be used (Doughty et al., 2013; Bearup et al., 2016).

References

Ahmed, D., Ansari, A., Imran, M., Dingle, K., and Bonsall, M. (2021a). Mechanistic modelling of covid-19 and the impact of lockdowns on a short-time scale. *PLOS ONE*, 16(e0258084).

Ahmed, D., Bailey, J., Petrovskii, S., and Bonsall, M. (2021b). *Mathematical Bases for 2D Insect Trap Counts*

Modelling, chapter In: Pham, T.D., Yan, H., Ashraf, M.W., Sjberg, F. (Eds.), Advances in Artificial Intelligence, Computation, and Data Science, pages 133 – 159. Springer International Publishing, Cham.

Ahmed, D., Benhamou, S., Bonsall, M., and Petrovskii, S. (2020). Three-dimensional random walk models of individual animal movement and their application to trap counts modelling. *J. Theor. Biol.*, 524(7). 110728.

Ahmed, D. A., Beidas, A., Petrovskii, S. V., Bailey, J. D., Bonsall, M. B., Hood, A. S. C., Byers, J. A., Hudgins, E. J., Russell, J. C., Ruzickova, J., Bodey, T. W., Renault, D., Bonnaud, E., Haubrock, P. J., Soto, I., and Haase, P. (2023). Simulating capture efficiency of pitfall traps based on sampling strategy and the movement of ground-dwelling arthropods. *Methods in Ecology and Evolution*, 00:1 – 17. https://doi.org/10.1111/2041-210X.14174.

Allen, A. and Singh, N. (2016). Linking movement ecology with wildlife management and conservation. *Frontiers in Ecology and Evolution*, 3(155).

Andersen, M. (1991). Properties of some density-dependent integrodifference equation population models. *Math. Biosci.*, 104:135 – 157.

Aspillaga, E., Safi, K., Hereu, B., and Bartumeus, F. (2019). Modelling the three-dimensional space use of aquatic animals combining topography and eulerian telemetry data. *Methods Ecol. Evol.*, 10:1551 – 1557.

Auger-Méthé, M., C.C.S., C., Lewis, M., and Derocher, A. (2011). Sampling rate and misidentification of l and non-l movement paths: comment. *Ecology*, 92:1699 – 1701.

Bailey, J. (2023). An assessment of the contact rates between individuals when movement is modelled by a correlated random walk. *Theor. Ecol.*, 16:239 – 252.

Bailey, J., Wallis, J., and Codling, E. (2018). Navigational efficiency in a biased and correlated random walk model of individual animal movement. *Ecology*, 99(1):217 – 223.

Banks, J., Laubmeier, A., and Banks, H. (2020). Modelling the effects of field spatial scale and natural enemy colonization behaviour on pest suppression in diversified agroecosystems. *Agricultural and Forest Entomology 22, 3040*, 22:30 – 40.

Bartumeus, F. and Catalan, J. (2009). Optimal search behavior and classic foraging theory. *J. Phys. A: Math. Theor.*, 42(43):569 – 580.

Bartumeus, F., Da Luz, M., Viswanathan, G., and Catalan, J. (2005). Animal search strategies: A quantitative random-walk analysis. *Ecology*, 86(11):3078 – 87.

Bartumeus, F., Peters, F., Pueyo, S., Marras., and Catalan, J. (2003). Helical l walks: Adjusting searching statistics to resource availability in microzooplankton. *Proc. Natl. Acad. Sci.*, 100:12771 – 12775.

Bearup, D., Benefer, C., Petrovskii, S., and Blackshaw, R. (2016). Revisiting Brownian motion as a description of animal movement: a comparison to experimental movement data. *Methods Ecol. Evol.*, 7(12):1525 – 37.

Benhamou, S. (2006). Detecting an orientation component in animal paths when the preferred direction is individual-dependent. *Ecology*, 87(2):518 – 528.

Benhamou, S. (2007). How Many Animals Really Do the Lévy walk? *Ecology*, 88(8):1962 – 69.

Berg, H. (1983). *Random Walks in Biology.* Princeton University Press.

Blackburn, T., Pyek, P., Bacher, S., Carlton, J., Duncan, R., Jaro V., Wilson, J., and Richardson, D. (2011). A proposed unified framework for biological invasions. *Trends Ecol. Evol.*, 26:333 – 339.

Blomfield, A., Menez, R., and Wilby, A. (2023). Population synchrony indicates functional connectivity in a threatened sedentary butterfly. *Oecologia*, 201:979 – 989.

Bouin, E., Calvez, V., Meunier, N., Mirrahimi, S., Perthame, B., Raoul, G., and Voituriez, R. (2012). Invasion fronts with variable motility: Phenotype selection, spatial sorting and wave acceleration. *Comptes Rendus Math.*, 350:761 – 766.

Bouin, E., Chan, M., Henderson, C., and Kim, P. (2018). Influence of a mortality trade-off on the spreading rate of cane toads fronts. *Commun. Partial Differ. Equ.*, 43:1627 – 1671.

Bowler, D. and Benton, T. (2005). Causes and consequences of animal dispersal strategies: relating individual behaviour to spatial dynamics. *Biol. Rev.*, 80:205 – 225.

Breed, G., Severns, P., and Edwards, A. (2015). Apparent power-law distributions in animal movements can arise from intraspecific interactions. *Journal of the Royal Society Interface*, 12(103). 20140927.

Briski, E., Drake, D., Chan, F., Bailey, S., and MacIsaac, H. (2014). Variation in propagule and colonization pressures following rapid humanmediated transport: Implications for a universal assemblagebased management model. *Limnol. Oceanogr.*, 59:2068 – 2076.

Bullock, J., Kenward, R. E., and Hails, R. (2002). *Dispersal ecology.* Oxford, UK: Blackwell.

Butikofer, L., Jones, B., Sacchi, R., Mangiacotti, M., and Ji, W. (2018). A new method for modelling biological invasions from early spread data accounting for anthropogenic dispersal. *PLoS ONE*, 13(11). e0205591.

Cagnacci, F., Boitani, L., Powell, R., and Boyce, M. (2010). Animal ecology meets gps-based radiotelemetry: a perfect storm of opportunities and challenges. *Philos. Trans. R. Soc. B Biol. Sci.*, 365:2157 – 2162.

Choules, J. and Petrovskii, S. (2017). Which Random Walk is Faster? Methods to Compare Different Step Length Distributions in Individual Animal Movement. *Math. Model. Nat. Phenom.*, 12(2):22 – 45.

Chu, A., Huber, G., McGeever, A., Veytsman, B., and Yllanes, D. (2021). A random-walk-based epidemiological model. *Sci. Rep.*, 11(19308).

Cleasby, I., Wakefield, E., Bearhop, S., Bodey, T., Votier, S., and Hamer, K. (2015). Three-dimensional tracking of a wide-ranging marine predator: flight heights and vulnerability to offshore wind farms. *J. Appl. Ecol.*, 52(1474 – 1482).

Clobert, J., Danchin, E., Dhondt, A., and Nichols, J. (2001). *Dispersal*. Oxford University Press.

Codling, E. and Bode, N. (2016). Balancing direct and indirect sources of navigational information in a leaderless model of collective animal movement. *J. Theor. Biol.*, 394:32 – 42.

Codling, E., Plank, M., and Benhamou, S. (2008). Random walk models in biology. *J. R. Soc. Interface*, 5(25):813 – 834.

Cooper, N., Sherry, T., and Marra, P. (2014). Modeling three-dimensional space use and overlap in birds. *Auk*, 131:681 – 693.

Courchamp, F., Fournier, A., Bellard, C., Bertelsmeier, C., Bonnaud, E., Jeschke, J., and Russell, J. (2017). Invasion biology: Specific problems and possible solutions. *Trends in Ecol. and Evol.*, 32(1):13 – 22.

De Jager, M., Bartumeus, F., Klzsch, A., Weissing, F., Hengeveld, G., Nolet, B., Herman, P., and Van De Koppel, J. (2014). How superdiffusion gets arrested: ecological encounters explain shift from l to brownian movement. *Proc. R. Soc. B Biol. Sci.*, 281(20132605).

De Jager, M., Weissing, F., Herman, P., Nolet, B., and van de Koppel, J. (2012). Response to Comment on "Lévy Walks Evolve Through Interaction Between Movement and Environmental Complexity". *Science*, 335(6071):918.

De Knegt, H., Hengeveld, G., Van Langevelde, F., De Boer, W., and Kirkman, K. (2007). Patch density determines movement patterns and foraging efficiency of large herbivores. *Behav. Ecol.*, 18:1065 – 1072.

Diagne, C., Leroy, B., Vaissi, A., Gozlan, R., Roiz, D., Jari, I., Salles, J., Bradshaw, C., and Courchamp, F. (2021). High and rising economic costs of biological invasions worldwide. *Nature*, 592:571 – 576.

Doughty, C., Roman, J., and Faurby, S., e. a. (2016). Global nutrient transport in a world of giants. *Proceedings of the National Academy of Sciences of the USA*, 113(4):868 – 873.

Doughty, C., Wolf, A., and Malhi, Y. (2013). The legacy of the pleistocene megafauna extinctions on nutrient availability in amazonia. *Nature Geosci.*, 6:761 – 764.

Edwards, A., Phillips, R., Watkins, N., Freeman, M., Murphy, E., Afanasyev, V., et al. (2007). Revisiting Lévy flight search patterns of wandering albatrosses, bumblebees and deer. *Nature*, 449(7165):1044 – 1048.

Ellis, J., Petrovskaya, N., and Petrovskii, S. (2018). Effect of density-dependent individual movement on emerging spatial population distribution: Brownian motion vs Lévy flights. *J. Theor. Bio.*, 464:159 – 178.

Fofana, A. and Hurford, A. (2017). Mechanistic movement models to understand epidemic spread. *Philos. Trans. R. Soc. B Biol. Sci.*, 372(20160086).

Fraser, K., Davies, K., Davy, C., Ford, A., Flockhart, D., and E.G., M. (2018). Tracking the conservation promise of movement ecology. *Frontiers in Ecology and Evolution*, 6(150).

Grimm, V. and Railsback, S. (2005). *Individual-based Modeling and Ecology.* Princeton University Press.

Gurarie, E., Anderson, J., and Zabel, R. (2009). Continuous models of population-level heterogeneity inform analysis of animal dispersal and migration. *Ecology*, 90(2233 – 2242).

Gurarie, E. and Ovaskainen, O. (2013). Towards a general formalization of encounter rates in ecology. *Theor. Ecol.*, 6:189 – 202.

Hapca, S., Crawford, J., and Young, I. (2009). Anomalous diffusion of heterogeneous populations characterized by normal diffusion at the individual level. *Journal of the Royal Society Interface*, 6:111 – 122.

Hastings, A. (1996). Models of spatial spread: A synthesis. *Biol. Conserv.*, 78:143 – 148.

Hawkes, C. (2009). Linking movement behaviour, dispersal and population processes: is individual variation a key? *J. Anim. Ecol.*, 78:894 – 906.

Holmes, E. E., Lewis, M., Banks, J. E., and Veit, R. R. (1994). Partial differential equations in ecology: spatial interactions and population dynamics. *Ecology*, 75:17 – 29.

Hooten, M., Johnson, D., McClintock, B., and Morales, J. (2017). *Animal Movement: Statistical Models for Telemetry Data*. CRC Press, Boca Raton: CRC Press, 1st ed. edition.

Hui, C. and Richardson, D. (2017). *Invasion dynamics*. Oxford University Press, 1st ed. edition.

Humphries, N., Queiroz, N., Dyer, J., Pade, N., Musyl, M., Schaefer, K., et al. (2010). Environmental context explains Lévy and Brownian movement patterns of marine predators. *Nature*, 465(7301):1066 – 9.

Humphries, N., Weimerskirch, H., Queiroz, N., Southall, E., and Sims, D. (2012). Foraging success of biological l flights recorded in situ. *Proc. Natl. Acad. Sci.*, 109:7169 – 7174.

James, A., Plank, M., and Edwards, A. (2011). Assessing Lévy walks as models of animal foraging. *J. R. Soc. Interface*, 8(62):1233 – 1247. https://doi.org/10.1098/rsif.2011.0200.

Jansen, V., Mashanova, A., and Petrovskii, S. (2012). Comment on "Lévy walks evolve through interaction between movement and environmental complexity". *Science*. 335(6071):918.

Jeltsch, F., Bonte, D., Pe'er, G., Reineking, B., and Leimgruber, P. e. a. (2013). Integrating movement ecology with biodiversity research - exploring new avenues to address spatiotemporal biodiversity dynamics. *Mov Ecol*, 1(6).

Kareiva, P. (1983). Local movement in herbivorous insects: applying a passive diffusion model to mark-recapture field experiments. *Oecologia (Berlin)*, (56:234). https://doi.org/10.1007/BF00379695.

Kareiva, P. and Shigesada, N. (1983). Analyzing insect movement as a correlated random walk. *Oecologia*, 56(2 – 3):234 – 238.

Kawai, R. and Petrovskii, S. (2012). Multiscale properties of random walk models of animal movement: lessons from statistical inference. *Proc R Soc*, 468:1428 – 1451.

Keenan, V. and Cornell, S. (2021). Anomalous invasion dynamics due to dispersal polymorphism and dispersalreproduction trade-offs. *Proc. R. Soc. B Biol. Sci.*, 288(20202825).

Kot, M., Lewis, M., and van den Driessche, P. (1996). Dispersal data and the spread of invading organisms. *Ecology*, 77:2027 – 2042.

Kot, M. and Schaffer, W. (1986). Discrete-time growth-dispersal models. *Math. Biosci.*, 80:109 – 136.

Lewis, M., Neubert, M., Caswell, H., Clark, J., and Shea, K. (2006). *A Guide to calculating discrete-time invasion rate from data*, chapter Cadotte,M.W.,McMahon, S.M., Fukami, T., Eds. Conceptual Ecology and Invasion Biology: Reciprocal Approaches to Nature, pages 69 – 192. Springer.

Lewis, M., Petrovskii, S., and Potts, J. (2016). *The Mathematics Behind Biological Invasions*. Interdisciplinary Applied Mathematics. Springer International Publishing, Cham.

Lin, C. C. and Segel, L. A. (1974). *Mathematics applied to deterministic problems in the natural sciences*. New York, NY: Macmillan.

Lockwood, J., Hoopes, M., and Marchetti, M. (2013). *Invasion ecology*. Wiley-Blackwell, Chichester, 2nd ed. edition.

Lutscher, F. (2019). *Integrodifference Equations in Spatial Ecology*. Interdisciplinary Applied Mathematics. Springer International Publishing, Cham.

Miller, J., Adams, C., Weston, P., and Schenker, J. (2015). *Trapping of Small Organisms Moving Randomly. Principles and Applications to Pest Monitoring and Management.* United States: Springer. Springer briefs in ecology.

Morris, A., Brger, L., and Crooks, E. (2019). Individual variability in dispersal and invasion speed. *Mathematics*, 7:795.

Mundt, C., Sackett, K., Wallace, L., Cowger, C., and Dudley, J. (2009). Long-distance dispersal and accelerating waves of disease: empirical relationships. *Am. Nat.*, 173(4):456 – 466.

Nathan, R., Getz, W., Revilla, E., Holyoak, M. Kadmon, R., and Saltz, D. (2008). A movement ecology paradigm for unifying organismal movement research. *Proc Natl Acad Sci USA*, 105:19052 – 9.

Neubert, M., Kot, M., and Lewis, M. (1995). Dispersal and pattern formation in a discrete-time predator-prey model. *Theor. Pop. Biol. 48, 743*, 48:7 – 43.

Nolet, B. and Mooij, W. (2002). Search paths of swans foraging on spatially autocorrelated tubers. *J. Anim. Ecol.*, 71:451 – 462.

Okubo, A. (1980). *Diffusion and Ecological Problems: Mathematical Models.* Springer, Berlin.

Okubo, A. and Levin, S. (2001). *Diffusion and ecological problems: modern perspectives.* Berlin, Germany: Springer.

Petrovskii, S., Bearup, D., Ahmed, D., and Blackshaw, R. (2012). Estimating insect population density from trap counts. *Ecol. complexity*, 10:69 – 82.

Petrovskii, S. and Morozov, A. (2009). Dispersal in a statistically structured population: fat tails revisited. *Am. Nat.*, 173(2):278 – 289.

Petrovskii, S., Petrovskya, N., and Bearup, D. (2014). Multiscale approach to pest insect monitoring: random walks, pattern formation, synchronization and networks. *Phys. Life Rev.*, 11(3):467 – 525.

Plank, M. and Codling, E. (2009). Sampling rate and misidentification of l and non-l movement paths. *Ecology*, 90:3546 – 3553.

Pyek, P., Hulme, P., Simberloff, D., Bacher, S., Blackburn, T., Carlton, J., Dawson, W., Essl, F., Foxcroft, L., Genovesi, P., Jeschke, J., Khn, I., Liebhold, A., Mandrak, N., Meyerson, L., Pauchard, A., Pergl, J., Roy, H., Seebens, H., Van Kleunen, M., Vil., Wingfield, M., and Richardson, D. (2020). Scientists warning on invasive alien species. *Biol. Rev.*, 95:1511 – 1534.

Reynolds, A. (2010). Bridging the gulf between correlated random walks and l walks: autocorrelation as a source of l walk movement patterns. *J R Soc Interface*, 7:1753 – 1758.

Reynolds, A. (2014). Mussels realize weierstrassian l walks as composite correlated random walks. *Scientific reports*, 4(1). 4409.

Reynolds, A. (2018). Current status and future directions of Lévy walk research. *Biology Open*. Published by The Company of Biologists Ltd.

Rodrigues, L., Mistro, D., Cara, E., Petrovskaya, N., and Petrovskii, S. (2015). Patchy Invasion of Stage-Structured Alien Species with Short-Distance and Long-Distance Dispersal. *Bull. Math. Biol.*, 77(8):1583 – 619.

Sandefur, J. (2018). A unifying approach to discrete single-species populations models. *Discrete and Continuous Dynamical Systems - Series B*, 23:493 – 508.

Shaw, M. (1995). Simulation of population expansion and spatial pattern when individual dispersal distributions do not decline exponentially with distance. *Proc. R. Soc. Lond. B Biol. Sci.*, 259:243248.

Shigesada, N. and Kawasaki, K. (1997). *Biological invasions: theory and practice*. Oxford University Press, Oxford.

Simberloff, D. (2013). *Invasive Species: What Everyone Needs to Know*. Oxford University Press., 1st ed. edition.

Sims, D., Humphries, N., Hu, N., Medan, V., and Berni, J. (2019). Optimal searching behaviour generated intrinsically by the central pattern generator for locomotion. *eLife*, 8(e50316).

Skarpaas, O. and Shea, K. (2007). Dispersal patterns, dispersal mechanisms, and invasion wave speeds for invasive thistles. *The American Naturalist*, 170(3):421 – 430.

Skellam, J. (1973). *The formulation and interpretation of mathematical models of diffusionary processes in population biology*. Academic Press, London, in: bartlett, m.s., hiorns, r.w. (eds.), the mathematical theory of the dynamics of biological populations edition. pp. 63 – 85.

Soto, I., Balzani, P., Carneiro, L., Cuthbert, R. N., Macedo, R., Tarkan, A. S., and Haubrock, P. J. e. a. (2023). Taming the terminological tempest in invasion science. https://doi.org/10.32942/X24C79.

Tracey, J., Sheppard, J., Zhu, J., Wei, F., Swaisgood, R., and Fisher, R. (2014). Movement-based estimation and visualization of space use in 3d for wildlife ecology and conservation. *PLoS ONE*, 9(7). e101205.

Turchin, P. (1998). *Quantitative analysis of movement. Measuring and modelling population redistribution in animals and plants.* Sinauer Associates, Inc. Sunderland, Massachusetts.

Viswanathan, G., Afanasyev, V., Buldryrev, S., Havlin, S., da Luz, M., R., and Stanley, H. (2000). Levy flights in random searches. *Physica*, 282:1–12.

Viswanathan, G., Afanasyev, V., Buldryrev, S., Havlin, S., da Luz, M., R., and Stanley, H. (2011). *The Physics of Foraging*. Cambridge University Press.

Williams, H., Taylor, L., Benhamou, S., Bijleveld, A., Clay, T., de Grissac, S., Demar, U., English, H., Franconi, N., GLaich, A., Griffiths, R., Kay, W., Morales, J., Potts, J., Rogerson, K., Rutz, C., Spelt, A., Trevail, A., Wilson, R., and Brger, L. (2020). Optimising the use of biologgers for movement ecology research. *Journal of Animal Ecology*, 89:186 – 206.

Wilson, R., Shepard, E., and Liebsch, N. (2008). Prying into the intimate details of animal lives: use of a daily diary on animals. *Endang. Species. Res.*, 4:123 – 137.

Zurell, D., Berger, U., Cabral, J., Jeltsch, F., Meynard, C., Mnkemller, T., Nehrbass, N., Pagel, J., Reineking, B., Schrder, B., and Grimm, V. (2010). The virtual ecologist approach: simulating data and observers. *Oikos*, 119:622 – 635.